J Solid State Electrochem (2012) 16:1291–1299
DOI 10.1007/s10008-011-1518-1

ORIGINAL PAPER

Electroless deposition of gold into poly-3,4-ethylenedioxythiophene films and their characterization performed in chloride-containing solutions

Veniamin V. Kondratiev · Nadejda A. Pogulaichenko · Suo Hui · Elena G. Tolstopjatova · Valery V. Malev

Received: 17 February 2011 / Revised: 30 June 2011 / Accepted: 29 July 2011 / Published online: 17 August 2011
© Springer-Verlag 2011

Abstract Au-containing polymer films were obtained by electroless deposition of gold from diluted solutions of $HAuCl_4$ into preliminarily reduced poly-3,4-ethylenedioxythiophene (PEDOT) films. Structural peculiarities of such pristine and composite films were characterized by scanning and transmission electron microscopy methods. It was established that the gold clusters forming under such deposition appear on the outer surface of polymer films and their pores. The clusters' sizes ranged between 30 and 100 nm depending on the time of exposition of a PEDOT film in solutions of Au(III) ions and the concentration of these ions. It was also observed that in contrast to pristine PEDOT films, cyclic voltammograms (CVs) of composite films in the presence of chloride ions show additional redox peaks resulting from oxidation of gold with formation of an insoluble product and followed by the product reduction under reversal of the potential scan direction. As a result of parallel electrochemical quartz crystal microbalance (EQCM) and CV measurements, it was also established that the number of chloride ions per one transferring electron in the gold oxidation process is near to unity. To elucidate the oxidation degree of gold in the presence of chloride ions, a special procedure of changing the electrode potential was used. It consisted of clamping the high anodic potential in the region of gold oxidation (0.97 V, Ag/AgCl) and subsequent gradual decrease of the electrode potential with a constant scan rate. Under these conditions, it was possible to completely oxidize all the gold particles containing in a composite film and find out the maximum amount of electricity consumed for the product particles' reduction. A comparison between such data and the results obtained in EQCM determinations of the gold content in the same film led to the conclusion that the oxidation state of gold in the complexes formed is Au(III). The effects of chloride ion concentration and scan rate of the electrode potential on current responses of PEDOT–Au films were investigated. Some primary conclusions on the kinetics of the studied processes are made.

Keywords Conducting polymers · Poly-3,4-ethylenedioxythiophene · Cyclic voltammetry · Transmitting electron microscopy · Electrochemical quartz crystal microbalance · Gold particles · Composite materials

V. V. Kondratiev (✉) · N. A. Pogulaichenko · E. G. Tolstopjatova · V. V. Malev
Department of Chemistry, Saint Petersburg University, Petrodvoretz, Universitetsky pr.26, 198504 Saint Petersburg, Russian Federation
e-mail: vkondratiev@mail.ru

S. Hui
State Key Laboratory on Integrated Optoelectronics, College of Electronic Science and Engineering, Jilin University, 2699 Qianjin Street, Changchun 130012, People's Republic of China

V. V. Malev
Institute of Cytology, Russian Academy of Sciences, 194064, Tikhoretsky pr. 4, Saint Petersburg, Russian Federation

Introduction

In recent years, much attention has been paid to studies of composite materials based on conducting polymers with metal clusters, in particular, gold and silver nanoparticles, incorporated into polymer matrix [1–24]. Among these new materials available for electroanalysis and electrocatalysis, poly-3,4-ethylenedioxythiophene (PEDOT) is one of the most promising conductive polymers with high electrical conductivity and stability of electrochemical responses.

Incorporation of gold and silver nanoparticles into PEDOT films was studied in [1–13] and [22–24], respectively. The following basic methods of such incorporation are commonly used: (1) incorporation of an electropositive metal into primarily reduced films due to redox interactions, (2) electrochemical deposition of a metal, and (3) incorporation of metal nanoparticles into a film during electropolymerization by uptake of stabilized colloid metal particles. In some cases, syntheses of metal composite films can be performed with using anodic dissolution of a metal electrode covered with an electroactive polymer and immersed into a solution containing ligands, which facilitate this anodic process. The metal complexes generated in result of the process are then reduced up to metal particles under either the subsequent application of cathodic polarizations or reversal of the potential scan direction. This way was used in [17, 18] to form gold-containing films of polyaniline.

The formation of PEDOT–Au composites resulting from the reduction of Au(III) ions by reduced fragments of PEDOT was studied by us earlier [12]. It was concluded that properties of such composite films can easily be controlled by varying the concentration of gold(III) ions, the time of exposition, and the initial potential of pristine PEDOT films. In the present work, PEDOT-based composite films, containing particles of gold, were also obtained by the first method, i.e., redox interaction of gold ions with preliminarily reduced fragments of the polymer. In our opinion, this electroless method of the metal particles' incorporation into conducting polymers has some advantages, as will be explained in the main part of the paper. The work also contains the results of electrochemical quartz crystal microbalance (EQCM) and electrochemical studies of such composite films in pure solutions of 0.1 M H_2SO_4 and mixed ones of 0.1 M H_2SO_4 with addition of small concentrations of chloride ions. As the results mainly concerning EQCM measurements with composite PEDOT–Au films were discussed in [12], these data are below mentioned without details, and the main focus of the paper is directed at new results.

We consider the oxidation/reduction processes at PEDOT/Au electrodes in chloride-containing solutions as representative test reactions, which allow one to judge on electrochemical properties of the electrodes under consideration. Besides, the electrochemical behavior of metal nanoparticles in porous conductive matrices is also of interest, since such reactions are increasingly used in different devices, including batteries and electrocatalytical systems. The paper also includes the results of scanning and transmission electron microscopy (SEM and TEM, respectively) studies of the composite films in question, which allowed us to judge about sizes of the gold clusters deposited in PEDOT films, as well as the film and cluster structures.

Experimental

Potentiostat AUTOLAB PGSTAT-30 (ECO CHEMIE, Netherlands) was used for the electrochemical deposition of PEDOT films onto conducting substrates and voltammetric measurements. The potential sweep rates in cyclic voltammogram (CV) measurements were 5–150 mV s^{-1}. Electrochemical measurements were performed in a three-electrode glass cell by using glassy carbon (GC) electrode (S=0.06 cm^2), platinum wire as an auxiliary electrode, and saturated silver chloride reference electrode. The GC electrode was polished to a mirror finish using alumina powder and then washed with deionized water prior to use.

Syntheses of PEDOT films were performed by electrodeposition under galvanostatic conditions ($j \approx 1$ mA cm^{-2}), and the range of potential variations was 1.3–1.0 V. The solutions that were used contained 0.05 M 3,4-ethylenedioxythiophene (EDOT, Aldrich), 0.5 M lithium perchlorate ($LiClO_4$, reagent grade) in acetonitrile purified cryogenically (HPLC grade, Cryochrom, Russia, water content below 0.05%). The resulting thickness of the synthesized PEDOT films was in the range of 0.2–1.3 μm. It was calculated basing on the polymerization charge (millicolumbs per square centimeter), assuming 2.25 electrons per monomer and a film density of about 1 g cm^{-3} [25].

Solutions of $HAuCl_4$ in 0.1 M H_2SO_4 were used for loading metallic gold into the films. The loading process was carried out through the reduction of the PEDOT film under constant potential at −0.3 V in supporting electrolyte solution (0.1 M H_2SO_4) followed by its immersion into $HAuCl_4$ solution (5×10^{-5}–5×10^{-3} M) in 0.1 M H_2SO_4. The time of the film reduction and the loading time were varied in the range of 60–300 s. All measurements were performed at room temperature (20±2 °C).

Electrochemical measurements with the rotating disk electrode (RDE) were carried out on a VED-06 instrument (Volta Ltd., Russia) with the rotation rate equal to 1,000 rpm. EQCM measurements were performed on a 5-MHz Pt-sputtered quartz crystals (S=1.37 cm^2). In our EQCM study of composite films, we used a PI-50-1 potentiostat equipped with a PR-8 programmer, a QCM100 quartz crystal microbalance analog controller combined with a QCM25 crystal oscillator (Stanford Research Systems, USA), and a computer-controlled frequency meter MXC1600 (Metex, Korea). We recorded simultaneously a cyclic voltammogram and the resonant frequency of the crystal oscillations. The complex we used permits monitoring of viscoelastic properties by measuring parameter Vc, which is the voltage connected with the crystal resistance to mechanical vibration (Rm), using the relationship $Rm = 10{,}000\times10^{-Vc/5} - 75$. The resonant frequency shift as a function of the electrode weight was presumed linear at Vc>3.5 V. All EQCM measurements were

performed for thin films (less than 0.2 μm), so that the effect of viscoelasticity of the films studied was negligible [26].

Morphology of the synthesized PEDOT and PEDOT–Au films was characterized by using scanning electron microscopy (SUPA 40VP, Carl Zeiss, Germany) and transmission electron microscopy (LIBRA 200FE, Carl Zeiss, Germany). Energy-dispersive X-ray (EDX) analysis was performed with an energy-dispersive X-ray spectrometer Oxford Instruments X-act.

Results and discussion

Syntheses of PEDOT–Au composite films were performed by a two-step procedure consisting of the reduction of PEDOT film in supporting electrolyte solution (0.1 M H_2SO_4) followed by its immersion into solution, containing chloride complexes of gold. Interactions of gold(III) ions possessing a high oxidation potential with reduced fragments of PEDOT film cause their oxidation and formation of metal gold particles inside the film. The fact of inclusion of gold particles into PEDOT films with formation of PEDOT–Au composite films was confirmed by means of EDX analysis. Although the details of such syntheses were described earlier in [12], it is useful to summarize them here in order to underline obvious advantages of the method applied.

In aqueous solutions of electrolytes, cyclic voltammograms (CV curves) of GC electrodes modified with pristine PEDOT films have a rectangular shape corresponding to practically constant values of the so-called low-frequency capacity of the films, C_{lf}, in a wide range of the electrode potentials (see Fig. 1, curve 1). Moreover, the charging/discharge processes of these films are reversible and not accompanied with any additional processes; both the cathodic and anodic currents increase in proportion to the potential scan rates, which is the direct evidence of reversible film charging/

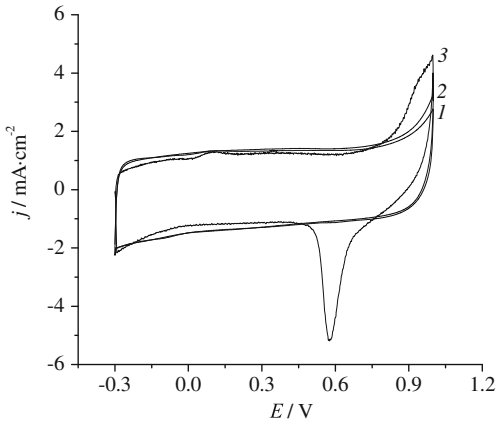

Fig. 1 CVs of pristine PEDOT film (*1*), composite PEDOT–Au film (*2*) in 0.1 M H_2SO_4 solution, and PEDOT–Au (*3*) in 0.1 M H_2SO_4+ 0.03 M NaCl solution (scan rate 50 mV s^{-1})

discharge processes [25–29]. Besides, PEDOT films show a stable electrochemical response in aqueous solutions of 0.1 M sulfuric acid. These circumstances permit one to estimate the amounts of gold deposited into PEDOT films under electroless reduction of $AuCl_4^-$ ions in result of the conjugated processes given below:

$$\mathrm{Au(III)} + 3\mathrm{e} \rightarrow \mathrm{Au}(0), \quad 3\mathrm{PEDOT} - 3\mathrm{e} \rightarrow 3\mathrm{PEDOT}^{+\cdot} \qquad (1)$$

Here, symbol PEDOT denotes a polymer fragment that might be oxidized to radical cation $PEDOT^{+\cdot}$. Its appearance should be compensated by either counter-ions moving in the film or delivery of electrons from the substrate surface, as it takes place under electroless deposition of metals.

We shall further assume the amounts of metal particles within a polymer film to be so small, that these species do not practically give any contribution to charging/discharge currents of the film. In these conditions, the resonant frequency curves of EQCM measurements should not change their shape (in function of the electrode potential) with increasing the metal deposited into the film. At the same time, the curves registered at different metal loadings must shift the more in the region of smaller resonant frequencies, the more the metal content of the film. To perform the corresponding estimates, one must equate two quantities, namely the amount of electricity consumed for deposition of some mass Δm_{Au} of gold and that given with the film under its discharge from initial potential E_i up to final one E_f, when the deposition process is interrupted. First quantity $Q_1 = 3F\frac{\Delta m_{Au}}{M_{Au}}$, where M_{Au}, the molar mass of gold, while second quantity $Q_2 = \int_{E_i}^{E_f} \frac{I\mathrm{d}E}{\nu} = \int_{E_i}^{E_f} C_{lf}\mathrm{d}E$, where ν is the scan rate. Thus, one obtains the following estimation of gold mass Δm_{Au} deposited into the film

$$\Delta m_{Au} = \frac{M_{Au}}{3F}\int_{E_i}^{E_f} C_{lf}\mathrm{d}E \approx \frac{M_{Au}C_{lf}}{3F}(E_f - E_i) \qquad (2)$$

Some inaccuracy of the obtained estimation might result from two following sources. First, mass Δm_{Au} determined from EQCM measurements should also reflect possible changes of the solvent content that occur during the gold deposition into the film. Spontaneous drift of the electrode potential due to the oxygen electroreduction might be the second source of possible errors. Obviously, potential E_f corresponding to the end of electroless deposition should be chosen in the range, where the rate of variations of the electrode potential is sufficiently high, in order to avoid possible errors in values of Q_2. In any case, a good accuracy of the above estimates was established for electroless palladium deposition into PEDOT films by comparing direct determinations of Δm_{Pd} and its calcula-

tions performed according to a relevant analog of Eq. 2 [30]. Thus, one can simply estimate the amounts of electropositive metals deposited into PEDOT films by registering time-dependent changes of the electrode potential during the deposition process and using CV data of pristine PEDOT films. We repeatedly applied this approach in this study but primarily examined its validity by using direct EQCM measurements of film mass increases at consecutive loadings of the same film with gold particles. The results of such an examination will be given below.

CV curves of GC electrodes modified with pristine PEDOT and composite PEDOT–Au films in 0.1 M H_2SO_4 show that oxidation and reduction currents of both films practically coincide in the potential range from −0.3 to 0.9 V (Fig. 1, curves 1 and 2). This means that in the case of composite films, the passing currents are also determined only by the film charging/discharge processes. Thus, gold particles do not take part in the redox processes in sulfuric acid solutions, the fact of which creates necessary premises for using the above estimations.

With an increase of the potential cycling range of composite PEDOT–Au films up to 1.3 V in 0.1 M H_2SO_4, the appearance of the anodic oxidation of gold with formation of Au_2O_3 ($E_{p,a}$=1.3 V) and the cathodic reduction of such product ($E_{p,c}$=0.9 V) were observed [12, 31]. Introduction of chloride ions into the bathing electrolyte caused the appearance of a new couple of redox processes at less positive potentials; the anodic shoulder of the gold chloride complexes formation at E≈0.9 V and the cathodic peak of their decomposition at E≈0.6 V (see Fig. 1, curve 3). To eliminate a possible formation of two products of the gold oxidation, the range of potential cycling was limited to 1 V further on.

It should be noted that a large difference between the potentials of the maximum cathodic and anodic currents is observed in CVs of composite films (see Fig. 1, curve 3), which can be interpreted as irreversibility of the oxidation/reduction processes with participation of metallic gold and the product of its oxidation in the presence of chloride ions. The performed comparison between integrals $Q_a = \int_{E_0}^{E'(0)} [j_a(E) - j_f(E)]dE$ and $Q_c = \int_{E(0)}^{E_0} [j_c(E) - j_f(E)]dE$, which are proportionate to the amounts of electricity consumed for the gold oxidation and its product reduction, respectively, showed that these quantities coincide each other with the accuracy of 10%. In these integrals, j_a and j_c are the anodic and cathodic currents of a composite PEDOT–Au film; j_f is the current of the same (pristine) film before its loading with gold particles; $E(0)$ and $E'(0)$ are cathodic and anodic limits of cycling the electrode potential; and E_0≈0.74 V is the electrode potential corresponding to zero rates of the anodic and cathodic processes: $j_a(E_0)-j_f(E_0)=j_c(E_0)-j_f(E_0)=0$. The determined values of Q_a occurred slightly decreased as compared to those of Q_c. This most probably resulted from some systematic errors in our determinations of currents $j_f(E)$ in the range of 0.9 V≤E≤1 V, where a more profound oxidation of pristine PEDOT films takes place (see curves 1 and 2 of Fig. 1). Thus, we established that the amounts of electricity consumed for the gold oxidation practically coincide with those required to reduce the products of such a process. It is also necessary to add that CVs measured in the presence of chloride ions are very stable at repeated potential cycling. These facts indicate a high stability of electrochemical properties of composite PEDOT–Au films and mean that products of the gold oxidation do not leave the film and thus are obviously insoluble.

CV curves of different electrodes of the same visible surface are represented in Fig. 2, which illustrates electrochemical properties of PEDOT–Au films (curve 3), polycrystalline gold electrode (curve 1), and golden aggregates electrodeposited onto the glassy carbon (GC–Au) surface (curve 2). As seen from Fig. 2, the currents associated with the gold chloride complexes formation and their reduction for PEDOT–Au electrode are much higher (approximately by five times) than those of GC–Au electrode. This, most likely, results from a small amount of gold aggregates on the electrode surface, since a very short time (about 3 s) was used for their electrodeposition in contrast to that took place in [32], where the electrodeposition time was equal to 60 s. However, the potentials of the maximum cathodic and anodic currents for the case of gold electrodeposited onto glassy carbon substrate are so close to those observed for PEDOT–Au electrode, that one can say about the evident resemblance between these electrodes. In the case of polycrystalline gold electrode, characteristic peaks of the corresponding redox processes are not seen due to the current density scale used in Fig. 2, though some

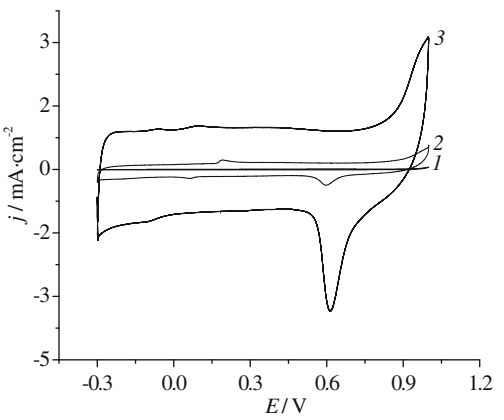

Fig. 2 CVs of compact gold electrode (*1*), GC electrode with a deposit of dispersed gold (*2*), and composite PEDOT–Au film (*3*) in 0.1 M H_2SO_4+0.02 M NaCl solution (scan rate 50 mV s^{-1})

increase in current values accompanied the transition from pure solutions of sulfuric acid to its mixed ones containing addenda of chloride ions. In other words, the polycrystalline gold electrode in essence behaves as a "real noble" metal and is practically inactive in chloride-containing solutions. This distinction of the golden electrode as compared to PEDOT–Au and GC–Au electrodes can be attributed to a higher activity of dispersed gold particles, in particular, a larger surface area of golden clusters in PEDOT–Au electrode. Thus, the observed difference in the electrochemical responses of the compared systems shows a strong influence of a dispersion state of metal particles on their electrochemical properties. The activity exhibited by golden clusters with respect to their oxidation in chloride-containing solutions seems reasonable from the positions of the mechanic chemistry developed recently in [33, 34]. At the same time, in case of PEDOT–Au films, one cannot exclude some initiating influence of the film matrix on the gold oxidation process, as it was observed for the same process in polyaniline films covering a polycrystalline gold electrode [17].

CVs of composite PEDOT–Au films recorded on RDE in chloride-containing solutions (see Fig. 3) were practically the same as those recorded on stationary electrodes. This means that diffusion of chloride ions in the bathing electrolyte is not a limiting step of the gold oxidation/reduction processes observed. Indeed, calculations of the limiting current densities resulted from the chloride ion diffusion to RDE by using the Levich equation:

$$J_{\text{lim}} = 0.62FD_{\text{Cl}}{}^{2/3}\upsilon^{-1/6}\omega^{1/2}C^{0}{}_{\text{Cl}}, \quad (4)$$

show that such densities are, at least, one order higher than the registered ones under the gold oxidation/reduction processes

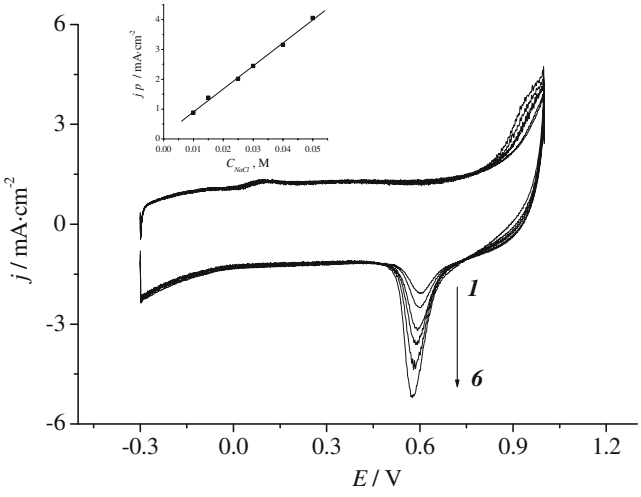

Fig. 3 CVs of composite PEDOT–Au film in 0.1 M H_2SO_4+x M NaCl solution on RDE (GC disk of 0.06 cm^2 in its area), where x, M: (*1*) 5×10^{-3}, (*2*) 1.5×10^{-2}, (*3*) 2.5×10^{-2}, (*4*) 3×10^{-2}, (*5*) 4×10^{-2}, and (*6*) 5×10^{-2}. On the *inset*: cathodic peak current j_p as a function of the NaCl concentration, ω=1,000 rpm, scan rate of 50 mV s^{-1}

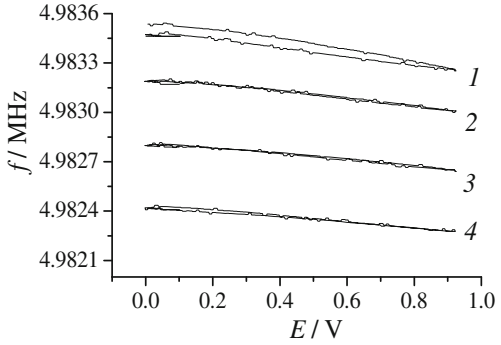

Fig. 4 Resonant frequency f as a function of cycling electrode potential E for PEDOT (*1*) and PEDOT–Au (*2–4*) films in 0.1 M H_2SO_4. *Curves 2–4* correspond to three consecutive loading of the same film with gold particles (scan rate, 10 mV s^{-1})

in PEDOT–Au films. In Eq. 4, D_{Cl} and υ are the diffusion coefficient of chloride ions and the kinematic viscosity, respectively; ω is the angular rotating velocity (ω is approximately equal to 100 rad s^{-1} in our measurements); and $C_{\text{Cl}}{}^{0}$ is the chloride ion concentration in the bathing solution.

Increasing the concentration of chloride ions in the bathing solution leads to the growth of the oxidation and reduction peaks recorded on PEDOT–Au electrode (see Fig. 4). In the range from 2×10^{-3} to 5×10^{-2} M Cl^- at constant potential (E=0.95 V), an increase of the gold oxidation currents in proportion to the chloride ion concentration was observed. This obviously points at the first order kinetics of the gold oxidation in the presence of chloride ions. The reverse process of reduction of the gold oxidation product also showed a proportional dependence of cathodic peak currents on the concentration of chloride ions in the same range of 2×10^{-3}–5×10^{-2} M Cl^- (see Fig. 4 and the inset). Subsequent increase of the concentration caused the appearance of a shoulder of the reduction peak, which might result from formation of another product of the gold oxidation.

One can assume that the observed formation of the gold oxidation product in the presence of chloride ions is mostly determined by a spatial distribution of gold particles within the film volume and their different accessibility for chloride ions due to possible diffusion limitations for ion transfer in the film bulk. Therefore, one could expect that CV curves recorded with different potential scan rates might reveal a strong dependence of the oxidation/reduction currents on the scan rate. This is observed only for low scan rates (up to 20 mV s^{-1}), but in the range 50–150 mV s^{-1}, the maximum currents are weakly dependent on the scan rate. These results point to a non-significant role of chloride ions diffusion limitations. This allows one to conclude that the process under consideration is limited with the step of the gold oxidation product formation.

A series of EQCM measurements were performed to determine the amounts of gold loaded into the films and stoichiometry of the gold oxidation/reduction processes. As it was expected (see above), the obtained curves reflecting dependencies of the resonant frequency of the PEDOT-coated quartz crystal on the electrode potential (*f*–*E*) with different amounts of loaded gold were parallel to each other and noticeably shifted to lower frequencies with increasing the amount of gold (see Fig. 4). The latter directly indicated at the growth of the film mass. It allowed us to estimate the amounts of metallic gold incorporated into PEDOT film by using the Sauerbrey equation. For three loadings repeated consecutively, the mass of the incorporated gold increased as follows: 4.5, 10.8, and 17.4 μg [12]. It was also found that such mass increases were proportional to the time of exposition of PEDOT film in the solution of Au(III) of a specified concentration.

We could also compare such mass increases with those followed from the above estimate basing on the Faraday law (see Eq. 2), since parallel measurements of changing the electrode potential in courses of the electroless gold deposition were performed (see Table 1).

As seen from the table, a good agreement between the results of both methods really takes place, though some decreases of the masses calculated according to Eq. 2 as compared to EQCM data are observed. These decreases, most likely, result from water flows accompanying the gold deposition into the film and thus increasing its weight.

Basing on the above results and assuming a layer-to-layer gold deposition, the number of gold monolayers that might be formed on the electrode surface was estimated. It turned out in the range of 20–40 layers, which indicates a spatial distribution of gold, at least in near-surface regions of the film. Such indirect conclusion is supported by the obtained SEM and TEM images of PEDOT composite films (see Figs. 5 and 6). As it is seen from the first figure, PEDOT films are some inhomogeneous formations including a large amount of pores, sizes of which are in the range of 50–200 nm. The deposited gold clusters are so large that their sizes lie in the range of 30–100 nm, depending on the concentration of Au (III) ions in the solution used for deposition and the duration of this process (see Fig. 6). A thorough examination of such TEM images shows that the gold clusters in most cases are covered with agglomerate structures formed by more small

Table 1 Comparison between the amounts of gold calculated from EQCM and CV data

Number	Δm, μg/cm^2 EQCM	Δm, μg/cm^2 CV
1	6.5	6.1
2	4.5	4.2
3	6.6	5.9

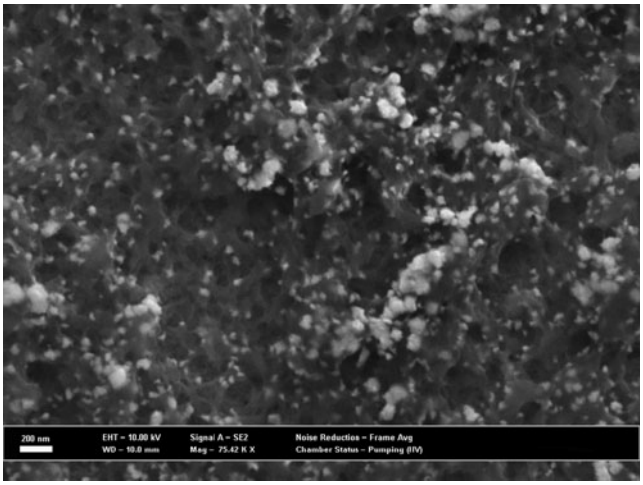

Fig. 5 SEM image of PEDOT–Au film. Time of gold loading was equal to 30 s in a 5×10^{-3} M $HAuCl_4$+0.1 M H_2SO_4 solution

metal particles, the diameters of which are about 10 nm (see inset in Fig. 6, where a single golden cluster of higher magnification is represented). From these data, it is now clear why we have not observed any diffusion limitations for the gold oxidation process. The films are porous; hence, the chloride ion's delivery to the surface of clusters is facilitated. The second important observation is in the established agglomerate structure of gold clusters, which also facilitates accessibility of gold particles to chloride ions and means that a reaction surface of gold clusters is significantly higher than the surface calculated from their diameters (30–100 nm, see above).

Dependencies of the mass changes of PEDOT–Au electrode resulting from the formation of gold oxidation product and its reduction in 0.1 M H_2SO_4 solutions with small addenda of chloride ions are represented in Fig. 7. As it is seen from the figure, a sudden decrease of the resonant frequency is observed on Δf–E curves for PEDOT–Au films during positive scan at $E\approx0.8$ V (i.e., the beginning of the process of gold oxidation). This is due to the corresponding

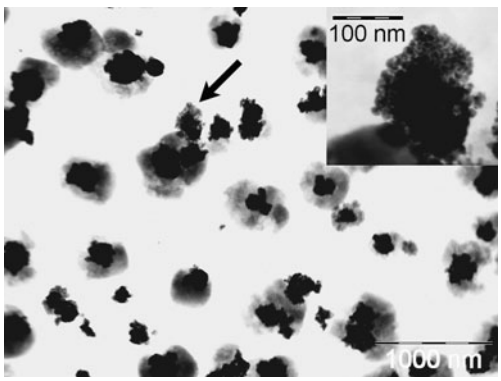

Fig. 6 TEM image of PEDOT–Au film. On the *inset*: single nanoparticle of gold, marked by *arrow*

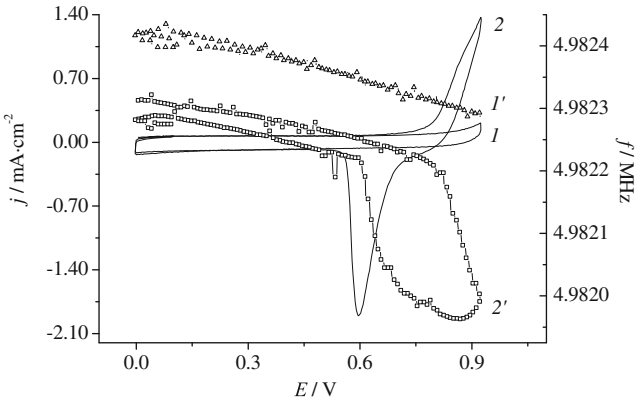

Fig. 7 CVs of pristine PEDOT film (*1*), composite PEDOT–Au film (*2*), and the resonant frequency as a function of potential *E* (*1′* and *2′*, respectively) in 0.1 M H_2SO_4+0.03 M NaCl solution (scan rate, 10 mV s^{-1})

increase of the film mass resulted from the formation of insoluble product of the gold oxidation with participation of chloride ions. On the reverse scan in the potential range, where the film oxidation is continuing (E=0.8–0.95 V), the resonant frequency keeps on decreasing and the film mass, thus, increases. On transition to the potential range of the product reduction (E=0.7–0.6 V), a sharp increase of the resonant frequency (i.e., a decrease of the electrode mass) is observed. It is consistent with the removal of chloride ions (and, probably, solvent molecules) into solution as a result of the product reduction process. It is worth noting that on continuous cycling of the electrode potential in the range of 0.0–0.95 V, a gradual increase of the composite film mass, which slowed down from cycle to cycle, was observed. The Δf–E curves become more stable with increasing the number of cycles, and the frequency dependency tips are locked that means the return of the film mass to its initial value. Continuous cycling of the electrode potential with low scan rate (10 mV s^{-1}) also leads to quasi-stationary conditions of the resonant frequency changes. These facts point at certain changes probably caused by gradual variations of the solvent content in the films studied.

Dependencies of the mass changes resulting from the gold oxidation product formation on the amount of electricity required for such process were plotted using the obtained data on voltammetry and frequency measurements. Close to linear dependencies of these mass changes on the amount of electricity consumed for the oxidation process (Δm vs ΔQ) were observed. These dependencies pointed at almost constant film mass gain in relation to the electricity consumed and allowed us to conclude that one stoichiometric product of the gold oxidation is predominantly formed under the conditions used. The molecular mass of the transferred particles participating in the formation of the oxidation product was calculated for a series of scanning cycles from slopes of Δm–ΔQ dependencies in the potential range of 0.80–0.95 V. The obtained values of an average molar mass of the particles transferred during the formation of this product are 56, 45, and 40 g mol^{-1} for 1st, 2nd, and 3rd cycles of scanning the potential, respectively. The last value of the molar mass is close to that of chloride ions, which means that one chloride ion is transferred per one consumed electron. A comparison between the amount of electricity required for oxidation of gold particles as obtained from CV data and that calculated according to Faraday's law for the mass of gold particles determined by EQCM (see above) showed that only 10–20% of the total gold loaded into the film can be oxidized during the anodic process in solutions containing the highest concentration (5×10^{-2} M) of chloride ions. To increase the part of the oxidized gold, we replaced the cyclic procedure of CV measurements with clamping the electrode potential at its high anodic value (0.97 V) in the range of the gold oxidation process and, after some variable time of such fixation, used a linear scanning of the potential in the cathodic direction. Under these conditions, the share of oxidized gold in the total gold content could be changed by varying the clamping duration. As a result of the above procedure, we hope to establish the nature of the insoluble product of gold oxidation thus formed by comparing the maximum amount of the product with the initial gold content in the film.

Current–voltage curves obtained at different durations of clamping the above anodic potential are represented in Fig. 8. One can see from the figure that such curves

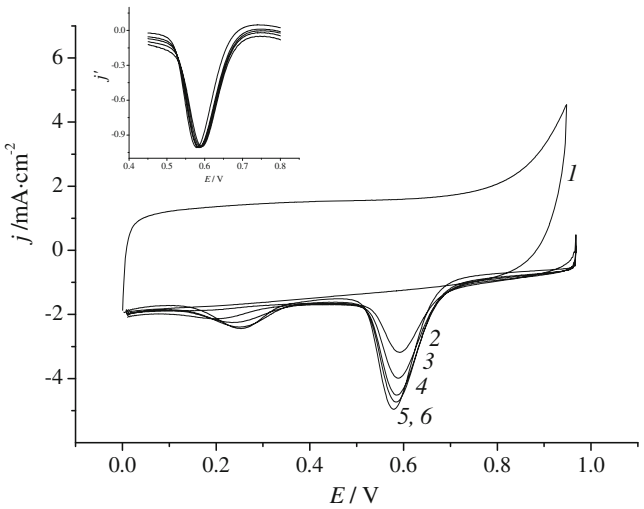

Fig. 8 CV for PEDOT–Au film in 0.1 M H_2SO_4 (*1*) and current–potential (*2–6*) dependencies for PEDOT–Au film in 0.1 M H_2SO_4+ 0.07 M NaCl solution, obtained at different durations of clamping the electrode potential at +0.97 V. Clamping duration, s: (*2*) 25, (*3*) 75, (*4*) 120, (*5*) 140, and (*6*) 280. On the *inset*: reduced cathodic current $j' = (j - j_f)/j_p$ as a function of electrode potential E; j_f, the capacity current of the pristine PEDOT film. Scan rate equals 50 mV s^{-1}. Time of gold loading was equal to 60 s in 1×10^{-3} M $HAuCl_4$+0.1 M H_2SO_4 solution. The film thickness $L\approx0.4$ μm

registered after large clamping durations (≥30 s) reveal two pronouncedly expressed peaks of the gold chloride complexes reduction. Thus, one can think that two products of the gold oxidation process are generated under the conditions indicated. As it was also established, the total amount of gold complexes implicated into the observed reduction processes became practically equal to the initial gold content in the used PEDOT film if sufficiently large durations of clamping the anodic potential (≥140 s) were applied. This conclusion was based on the established practical coincidence between the amount of electricity consumed for the gold deposition (i.e., amount $Q_2 = \int_{E_i}^{E_f} C_{lf} dE$, see above) and that required to reduce the gold complexes formed in result of the oxidation processes (the last amount (Q_3) was calculated as a sum of two areas corresponding to both cathodic peaks of the gold complexes reduction, see Fig. 8 and Table 2). This, in particular, means that the oxidation state of gold in the complexes formed is exactly Au(III).

In result of repeated recordings of cathodic curves registered after large clumping durations (≥140 s, see above), we established that in the case of using different films, the ratio of cathodic peak values corresponding to the presumed different products is an accidental value. Moreover, the second reduction peak (at approximately 0.25–0.3 V) disappears completely if the film thickness is sufficiently small (≤0.2 μm). However, such peak appears if the same thin film is covered with additional layers of the polymer due to its electropolymerization in EDOT solutions not containing gold ions (see Fig. 9). These findings allow one to reasonably think that the observed formation of the second gold oxidation product is only apparent. In our opinion, the appearance of the second reduction peak results from an embarrassing accessibility of some part of gold clusters for chloride ions. It seems verisimilar that such difficulties in accessibility of gold clusters for chloride ions must appear, when the thickness of an initially thin film is increased without accompanying gold deposition, as it was observed in the case of using the corresponding procedure applied to thin films (see above).

According to the explanation proposed, we suppose that in the course of gold deposition into PEDOT films, the formation of metal clusters mainly proceeds on the outer surface of the films and within their pores. One can also think that some part of the formed clusters occurs arduously accessible for chloride ions due to the elastic tensions arising in the film under an inevitable increase of its volume in the course of gold deposition. The analogous diffusion hindrances might appear in the course of the gold chloride complexes formation as a result of differences in the partial volume of gold atoms and that of the oxidation product molecules. It is also clear that the probability of finding such arduously accessible clusters is not an easily controlled property but must rise with increasing the film thickness, as it is observed in reality. Thus, in our opinion, the appearance of the second gold oxidation product has received a reasonable explanation, though the latter probably needs additional verifications.

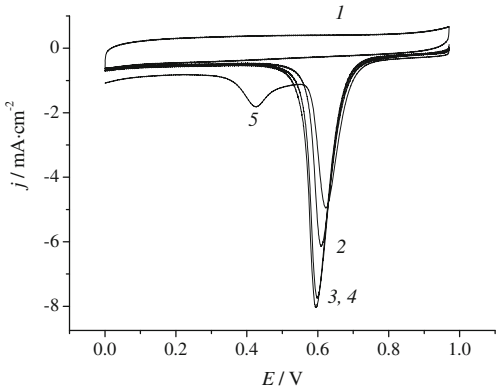

Fig. 9 CV for PEDOT–Au film in 0.1 M H_2SO_4 (*1*) and current–potential (*2–5*) dependencies for PEDOT–Au film in 0.1 M H_2SO_4+ 0.05 M NaCl solution, obtained at different durations of clamping the potential at +0.97 V. Clamping duration, seconds: (*2*) 50, (*3*) 220, (*4*) 360, and (*5*) 360. *Curve 5* corresponds to the same composite film, the initial thickness (L_1=0.2 μm) of which was increased by two times approximately without additional film loading with gold particles. Scan rate equals 50 mV s^{-1}. Time of gold loading was equal to 60 s in 1×10^{-3} M $HAuCl_4$+0.1 M H_2SO_4 solution

Another issue raised in the study concerns stoichiometric content of the complexes formed at the gold oxidation in the presence of chloride ions. By using data represented in Fig. 8, one can see that in the main region of the product reduction (at $E\approx0.6$ V), the reduced current curves $j(E)/j_p$ (here j_p, the cathodic peak current) have not changed their shape under increased clamping duration (see insert to Fig. 8). This most likely means that the kinetics of the gold complexes' reduction does not suffer any changes either. Taking into account the facts that in the process of gold oxidation the act of one-electron transfer is conjugated with delivery of one chloride ion and the oxidation state of gold is Au(III), one can think that neutral polynuclear complexes of general formula $AuCl_3$ are the predominant product of such oxidation at relatively low concentrations of chloride ions in the bathing solution. As for the reasons why the formed $AuCl_3$ particles do not react further with chloride ions forming soluble $AuCl_4^-$ ions, we can only suppose that outer

Table 2 Comparison between the amounts of electricity calculated from the Faraday law, Q_2, and the reduction process, Q_3

Number	Q_2, mC	Q_3, mC
1	7.16	6.97
2	7.06	7.52
3	6.99	8.69

layers of $AuCl_3$ particles surrounding metal clusters specifically interact with sulfur atoms of PEDOT polymer chains, and these interactions are stronger than those taking place for chloride ions. With respect to the inner $AuCl_3$ species, they most likely react with each other due to formation of metal–metal bonds, so that clusters of these species on the whole turn out stable.

Quantitative simulations of the oxidation/reduction processes studied in this work are in progress now, and their results will be published elsewhere.

Conclusions

PEDOT–Au composite films obtained by electroless deposition of gold from its solutions into preliminarily reduced pristine films were studied by different methods. The amounts of metal particles incorporated were determined in result of EQCM measurements. On the other hand, such quantities were calculated basing on the Faraday law. Both methods led to practically coinciding results. The obtained TEM images of composite films showed that gold particles incorporated in PEDOT films form agglomerate clusters of total radii in the range of 30–100 nm depending on the deposition conditions. It was also shown that in the CV curves of composite films, additional redox peaks resulting from the gold oxidation with formation of insoluble chloride complexes appear in the presence of chloride ions. The obtained results permit the conclusion that oxidation of dispersed gold particles in chloride-containing solutions leads to formation of polynuclear low soluble product, the most probable form of which is $AuCl_3$.

Acknowledgments The authors are thankful to Drs. Anton Bondarenko, Oleg Vyvenko, and Evgeny Ubyivovk for the help we have derived during common SEM and TEM measurements. We also thank the Russian Foundation for Basic Research (grants 07-03-00662 and 10-03-00793) and the St. Petersburg State University grant №12.38.15.2011 for financial maintenance of this work.

References

1. Zanardi C, Terzi F, Pigani L, Heras A, Colina A (2008) Electrochim Acta 53:3916–3923
2. Terzi F, Zanardi C, Martina V, Pigani L, Seeber R (2008) J Electroanal Chem 619–620:75–82
3. Mathiyarasu J, Senthilkumar S, Phani KLN, Yegnaraman V (2008) Mater Lett 62:571–573
4. Kim SY, Lee Y, Cho MS, Son Y, Chang JK (2007) Mol Cryst Liq Cryst 472:201–207
5. Harish S, Mathiyarasu J, Phani KLN (2009) Mater Res Bull 44:1828–1833
6. Manesh KM, Santhosh P, Gopalan A, Lee KP (2008) Talanta 75:1307–1314
7. Kumar SS, Mathiyarasu J, Phani KL (2005) J Electroanal Chem 578:95–103
8. Li X, Li Y, Tan Y, Yang C, Li Y (2004) J Phys Chem B 108:5192–5199
9. Selvaganesh S, Mathiyarasu J, Phani KLN, Yegnaraman V (2007) Nanoscale Res Lett 2:546–549
10. Kumar SS, Kumar CS, Mathiyarasu J, Phani KLN (2007) Langmuir 23:3401–3408
11. Lu G, Li C, Shen J, Chen Z, Shi G (2007) J Phys Chem C 111:5926–5931
12. Pogulaichenko NA, Hui S, Tolstopjatova EG, Malev VV, Kondratiev VV (2009) Russ J Electrochem 45:1176–1182
13. Kim BY, Cho MS, Kim YS, Son Y, Lee Y (2005) Synth Met 153:149–152
14. Huang X, Li Y, Chen Y, Wang L (2008) Sens Actuators B 134:780–786
15. Li J, Lin XQ (2007) Anal Chim Acta 596:222–230
16. Sarma TK, Chowdhury D, Paul A, Chattopadhyay A (2002) Chem Commun 10:1048–1049
17. Hatchett DW, Josowicz M, Janata J (1999) Chem Mater 11:2989–2994
18. Saheb A, Smith JA, Josowicz M, Janata J, Baer DR, Engelhard MH (2008) J Electroanal Chem 621:238–244
19. Panda BR, Chattopadhyay A (2007) J Colloid Interface Sci 316:962–967
20. Choudhury A (2009) Sens Actuators B 138:318–325
21. Song FY, Shiu KK (2001) J Electroanal Chem 498:161–170
22. Ocypa M, Ptasinska M, Michalska A, Maksymiuk K, Hall EAH (2006) J Electroanal Chem 596:157–168
23. Namboothiry MAG, Zimmerman T, Colder FM, Liu J, Kim K, Carroll DL (2007) Synth Met 157:580–584
24. Pacios R, Marcilla R, Pozo-Gonzalo C, Pomposo JA, Grande H, Aizpurua J, Mecerreyes D (2007) J Nanosci Nanotechnol 7:2938–2941
25. Bobacka J, Lewenstam A, Ivaska A (2000) J Electroanal Chem 489:17–27
26. Gustafson JC, Liedberg B, Inganas O (1994) Solid State Ionics 69:145–152
27. Eliseeva SN, Spiridonova DV, Tolstopyatova EG, Kondratiev VV (2008) Russ J Electrochem 44:894–900
28. Tolstopyatova EG, Pogulaichenko NA, Eliseeva SN, Kondratiev VV (2009) Russ J Electrochem 45:252–262
29. Eliseeva SN, Babkova TA, Kondratiev VV (2009) Russ J Electrochem 45:152–159
30. Eliseeva SN, Malev VV, Kondratiev VV (2009) Russ J Electrochem 45:1045–1051
31. Lai LJ, Yang YW, Lin YK, Huang LL, Hsieh YH (2009) Colloids Surf B 68:130–135
32. He X, Yuan R, Chai Y, Shi Y (2008) J Biochem Bioph Methods 70:823–829
33. Rusanov AI (2006) Thermodynamic foundations of mechanochemistry. Nauka, St. Petersburg
34. Rusanov AI, Ur'ev NB, Eryukin PV, Movchan TG, Esipova NE (2004) Dokl Phys Chem 395:88–90